

## **Supporting Information**

### **CO<sub>2</sub>-Switchable Hierarchically Porous Zirconium-Based MOF-Stabilized Pickering Emulsions for Recyclable Efficient Interfacial Catalysis**

Xiaoyan Pei\*, Jiang Liu, Wangyue Song, Dongli Xu, Zhe Wang and Yanping Xie  
*College of Chemistry and Chemical Engineering, Xinyang Normal University,  
Xinyang 464000, China.*

\* Correspondence: xiaoyanpei2009@163.com

Number of pages: 16

Number of figures: 28

Number of tables: 3

#### **Table of Contents**

1. Experimental section.....	S3
2. Figures S1-S28.....	S4
3. Tables S1-S3.....	S16

## 1. Experimental section

## Materials

ZrCl<sub>4</sub>, Zn(NO)<sub>3</sub>·6H<sub>2</sub>O, benzoic acid, 2,5-dihydroxyterephthalic acid, and 2,5-dihydroxyterephthalic acid were obtained from Aladdin. (3-Aminopropyl)trimethoxysilane (APTMS), 3-(2-aminoethylamino)propyltrimethoxysilane (AEAPTMS) and 3-[2-(2-aminoethylamino)ethylamino]propyl-trimethoxysilane (AEAEAPTMS) were obtained from Energy Chemical Co., Ltd. CO<sub>2</sub> (Praxair, SFC grade, 99.998 vol%) and N<sub>2</sub> (Praxair, 99.9993 vol%) were obtained from Praxair. All the chemicals were used as received unless otherwise stated.

## Instrumentation

X-ray photoelectron spectroscopy (XPS) were determined on a Thermo Scientific K-Alpha electron energy spectrometer using Al K $\alpha$  (1486.6 eV) as the X-ray source. X-ray diffraction (XRD) patterns were measured on a Rigaku SmartLab9 diffractometer with monochromatic Cu K $\alpha$  radiation ( $\lambda = 1.5418 \text{ \AA}$ ). Scanning electron microscopy (SEM) were recorded on a Hitachi S-4800 microscope at 5 kV. Nuclear magnetic resonance (NMR) spectra were carried out on a JNM-ECZ600R/S3 spectrometer (600 MHz). Mass spectra were measured on an Agilent GC-MS-5890A/5975C Plus spectrometer (EI). Water contact angles were obtained through a KRÜSS Drop Shape Analyzer 25 (KRÜSS DSA25).

## 2. Figures S1-S28

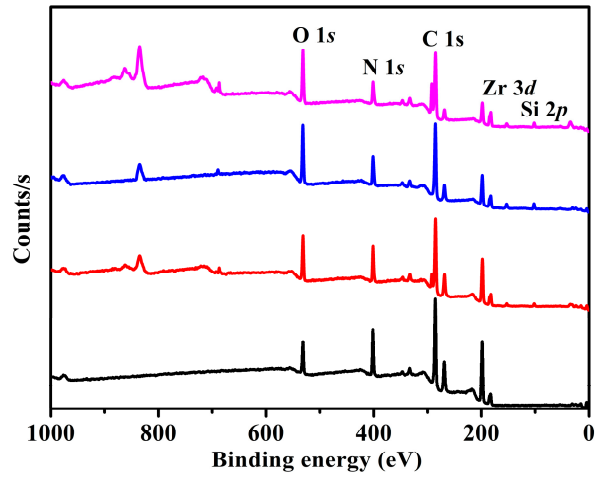


**Figure S1** XPS spectrum of (a) H-UiO-66-(OH)<sub>2</sub>, (b) H-UiO-66-(OAPTMS)<sub>2</sub>, (c) H-UiO-66-(OAEAPTMS)<sub>2</sub> and (d) H-UiO-66-(OAEAEAPTMS)<sub>2</sub>.

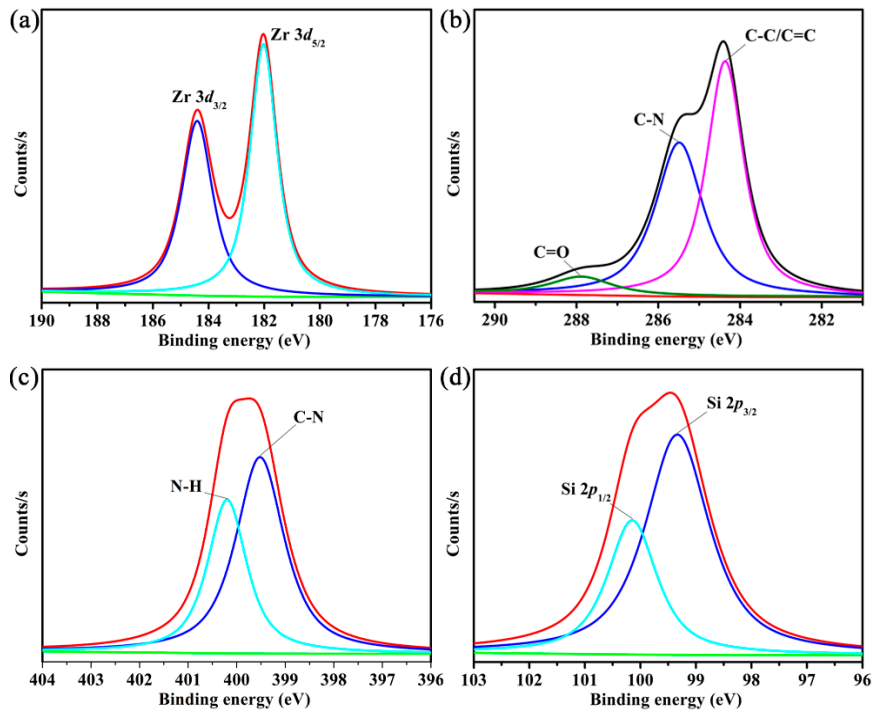


**Figure S2** High-resolution XPS spectrum of Zr 3d (a), C 1s (b), N 1s (c) and Si 2p (d) of H-UiO-66-(OAPTMS)<sub>2</sub>.

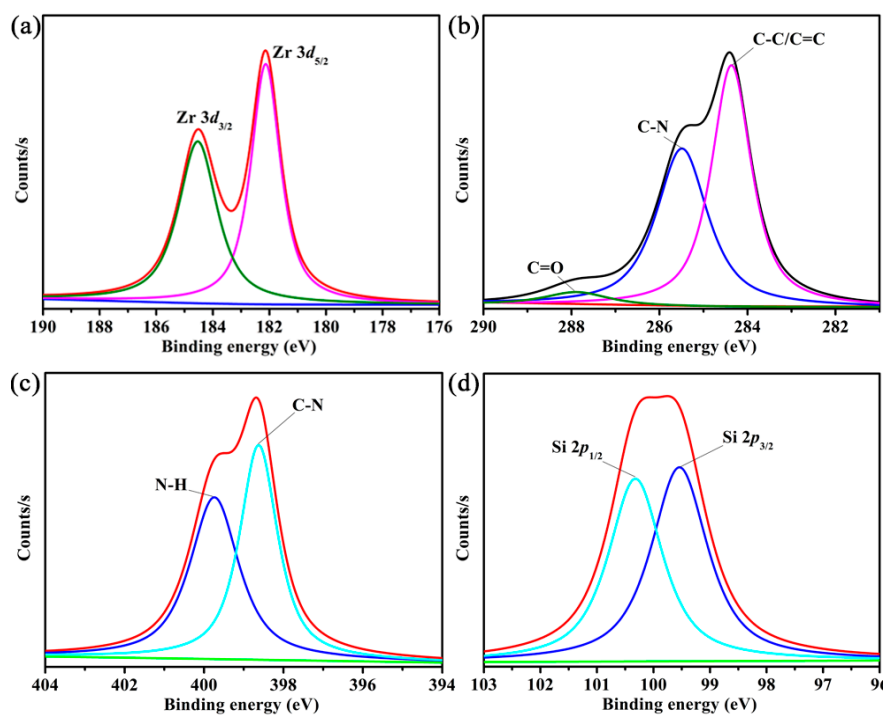


**Figure S3** High-resolution XPS spectrum of Zr 3d (a), C 1s (b), N 1s (c) and Si 2p (d) of H-UiO-66-(OAEAPTMS)<sub>2</sub>.

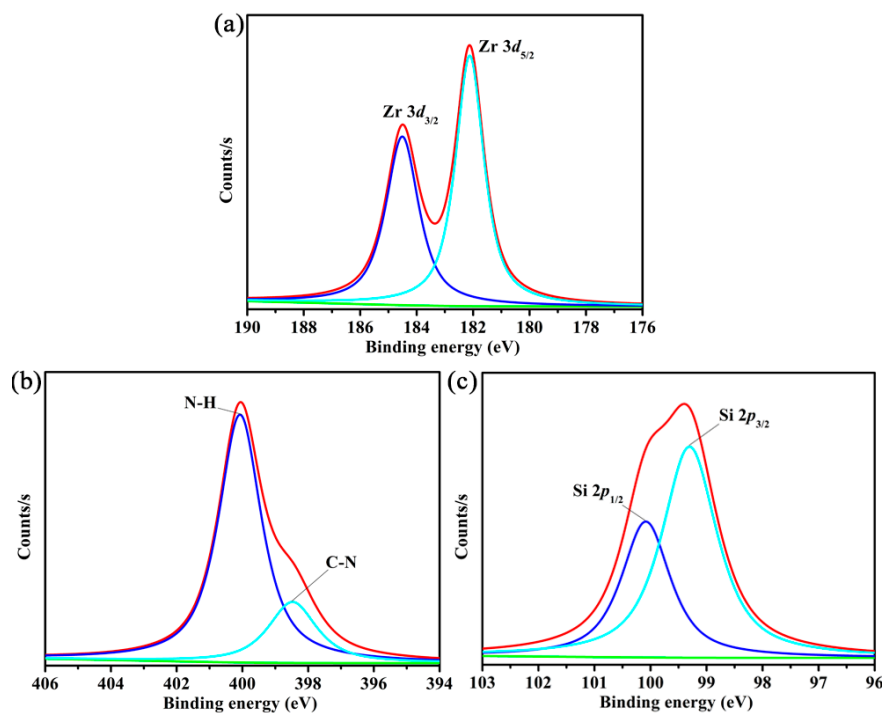


**Figure S4** High-resolution XPS spectrum of Zr 3d (a), N 1s (b) and Si 2p (c) of H-UiO-66-(OAEAPTMS)<sub>2</sub>.

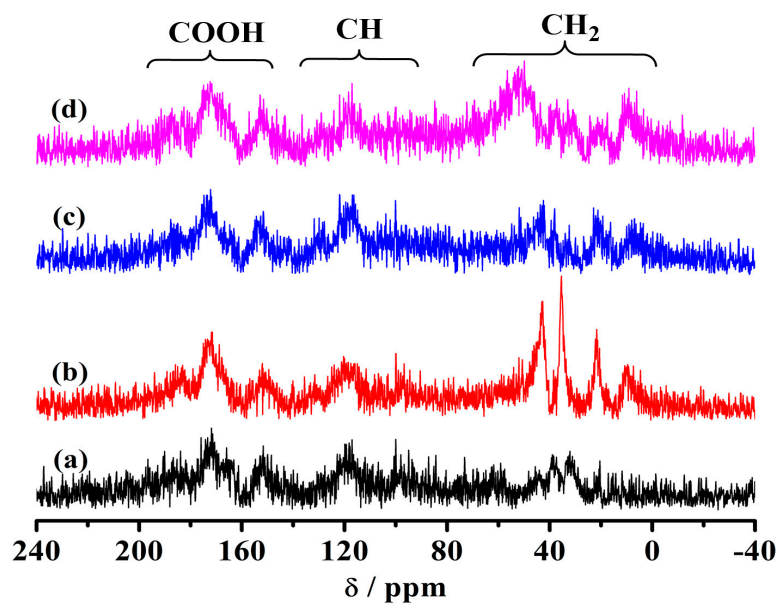


**Figure S5** Solid-state  $^{13}\text{C}$  NMR spectra of (a) H-UiO-66-(OH)<sub>2</sub>, (b) H-UiO-66-(OAPTMS)<sub>2</sub>, (c) H-UiO-66-(OAEAPTMS)<sub>2</sub> and (d) H-UiO-66-(OAEAEAPTMS)<sub>2</sub>.

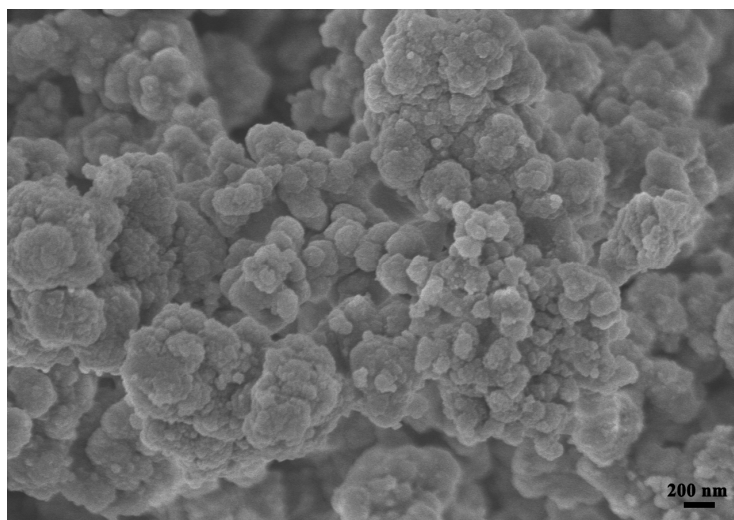


**Figure S6** SEM image of the pristine H-UiO-66-(OH)<sub>2</sub>.

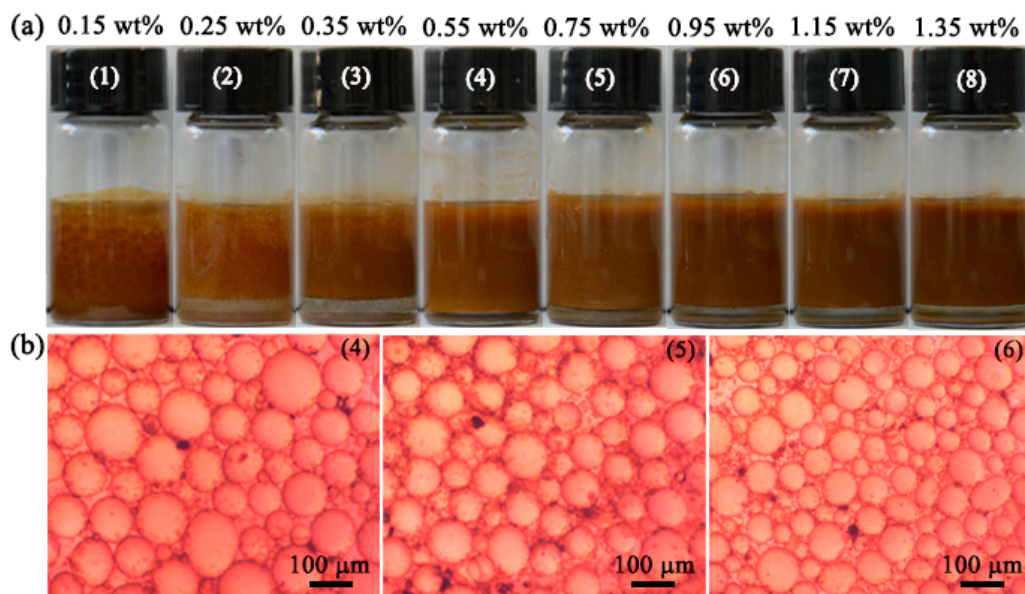


**Figure S7** Photographs of toluene-in-water emulsions stabilized by H-UiO-66-(OAPTMS)<sub>2</sub> (a) and chosen micrographs for (4), (5) and (6) in (a) (b).

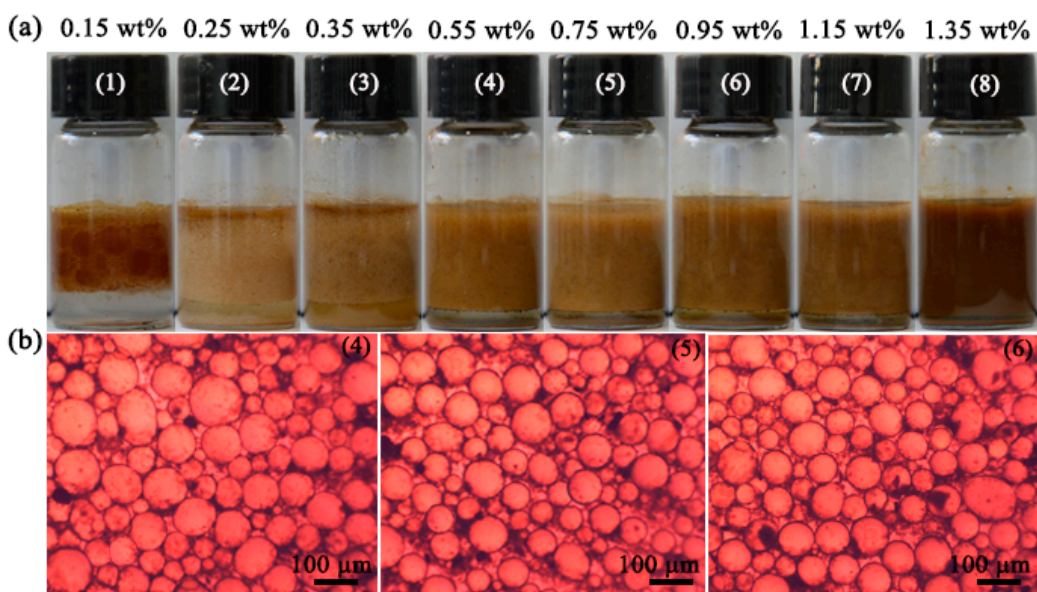


**Figure S8** Photographs of toluene-in-water emulsions stabilized by H-UiO-66-(OAEAPTMS)<sub>2</sub> (a) and chosen micrographs for (4), (5) and (6) in (a) (b).

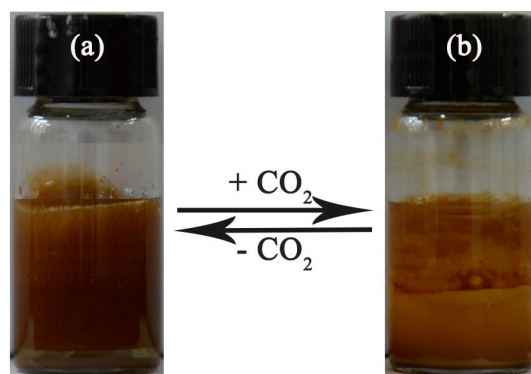


**Figure S9** Photographs of benzene (3 ml)-water (2 ml) emulsion stabilized by H-UiO-66-(OAPTMS)<sub>2</sub> (0.55 wt%): (a), before CO<sub>2</sub> bubbling; (b), after CO<sub>2</sub> bubbling.

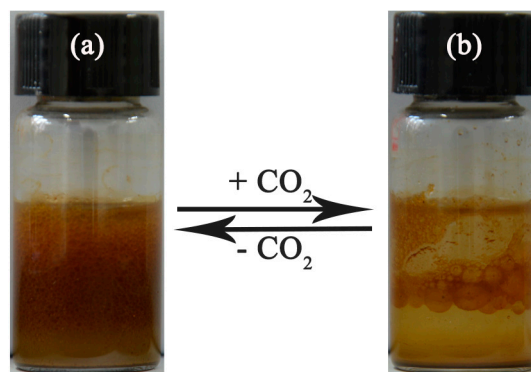


**Figure S10** Photographs of benzene (3 ml)-water (2 ml) emulsion stabilized by H-UiO-66-(OAEAPTMS)<sub>2</sub> (0.55 wt%): (a), before CO<sub>2</sub> bubbling; (b), after CO<sub>2</sub> bubbling.

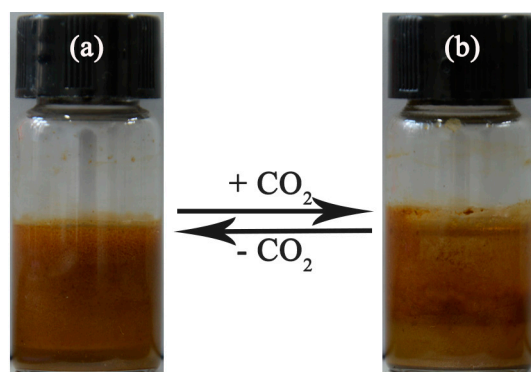


**Figure S11** Photographs of benzene (3 ml)-water (2 ml) emulsion stabilized by H-UiO-66-(OAEAEAPTMS)<sub>2</sub> (0.55 wt%): (a), before CO<sub>2</sub> bubbling; (b), after CO<sub>2</sub> bubbling.

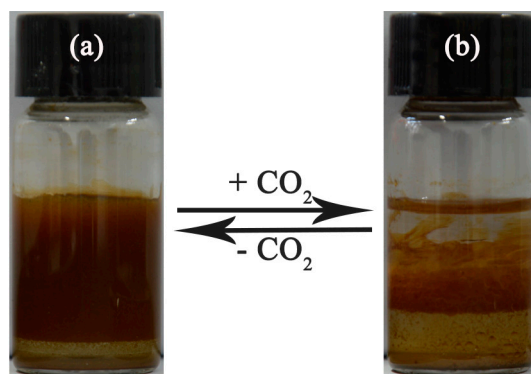


**Figure S12** Photographs of n-hexane (3 ml)-water (2 ml) emulsion stabilized by H-UiO-66-(OAPTMS)<sub>2</sub> (0.55 wt%): (a), before CO<sub>2</sub> bubbling; (b), after CO<sub>2</sub> bubbling.

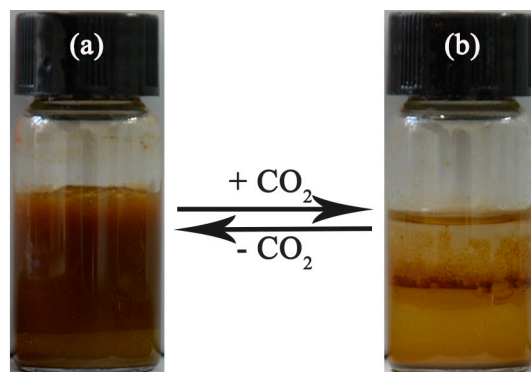


**Figure S13** Photographs of n-hexane (3 ml)-water (2 ml) emulsion stabilized by H-UiO-66-(OAEAPTMS)<sub>2</sub> (0.55 wt%): (a), before CO<sub>2</sub> bubbling; (b), after CO<sub>2</sub> bubbling.

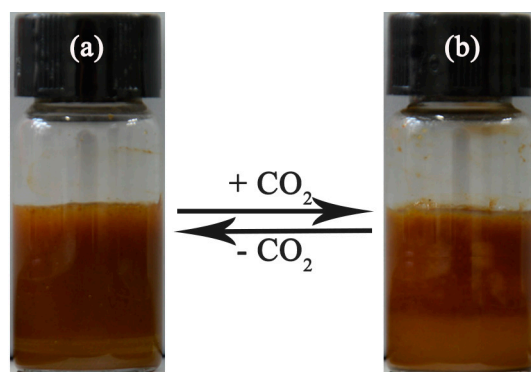


**Figure S14** Photographs of n-hexane (3 ml)-water (2 ml) emulsion stabilized by H-UiO-66-(OAEAEAPTMS)<sub>2</sub> (0.55 wt%): (a), before CO<sub>2</sub> bubbling; (b), after CO<sub>2</sub> bubbling.

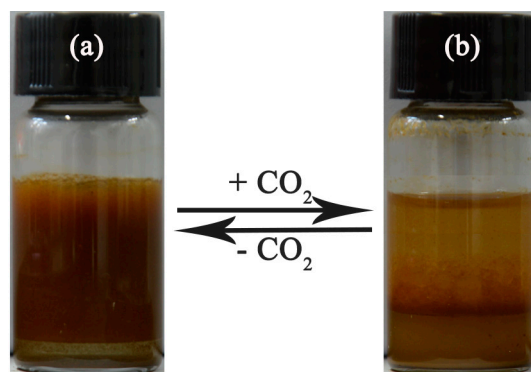


**Figure S15** Photographs of cyclohexane (3 ml)-water (2 ml) emulsion stabilized by H-UiO-66-(OAPTMS)<sub>2</sub> (0.55 wt%): (a), before CO<sub>2</sub> bubbling; (b), after CO<sub>2</sub> bubbling.

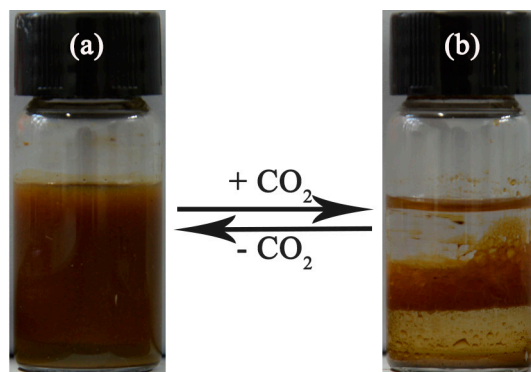


**Figure S16** Photographs of cyclohexane (3 ml)-water (2 ml) emulsion stabilized by H-UiO-66-(OAEPTMS)<sub>2</sub> (0.55 wt%): (a), before CO<sub>2</sub> bubbling; (b), after CO<sub>2</sub> bubbling.

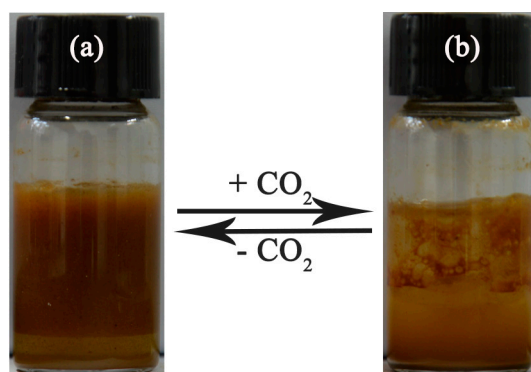


**Figure S17** Photographs of cyclohexane (3 ml)-water (2 ml) emulsion stabilized by H-UiO-66-(OAEAEPTMS)<sub>2</sub> (0.55 wt%): (a), before CO<sub>2</sub> bubbling; (b), after CO<sub>2</sub> bubbling.

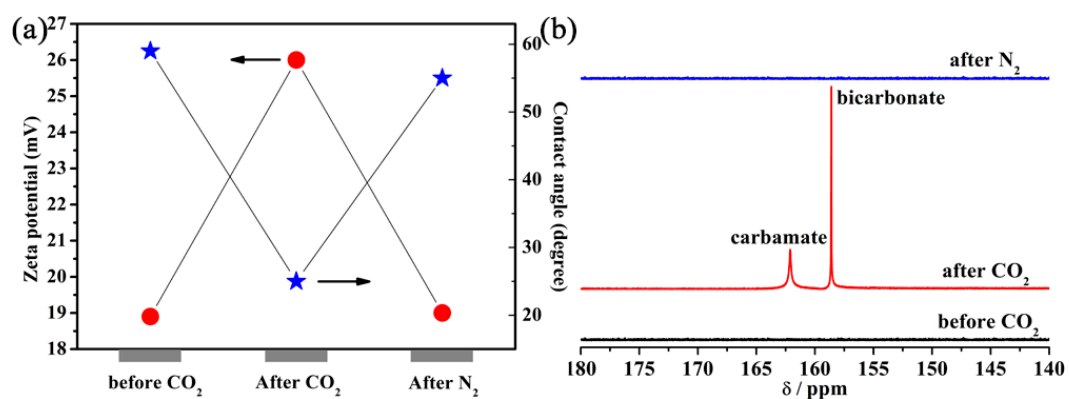


**Figure S18** Zeta potential and contact angle of H-UiO-66-(OAPTMS)<sub>2</sub> before CO<sub>2</sub>, after CO<sub>2</sub> and after N<sub>2</sub>.

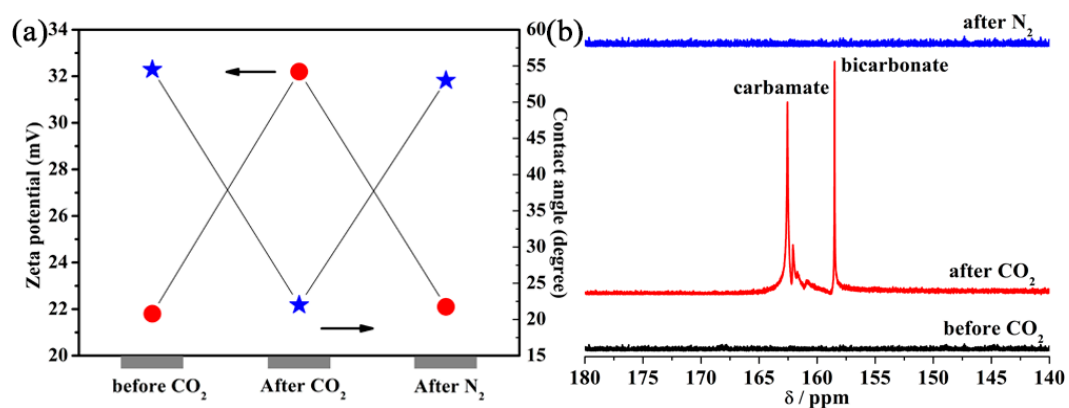


**Figure S19** Zeta potential and contact angle of H-UiO-66-(OAEAPTMS)<sub>2</sub> before CO<sub>2</sub>, after CO<sub>2</sub> and after N<sub>2</sub>.

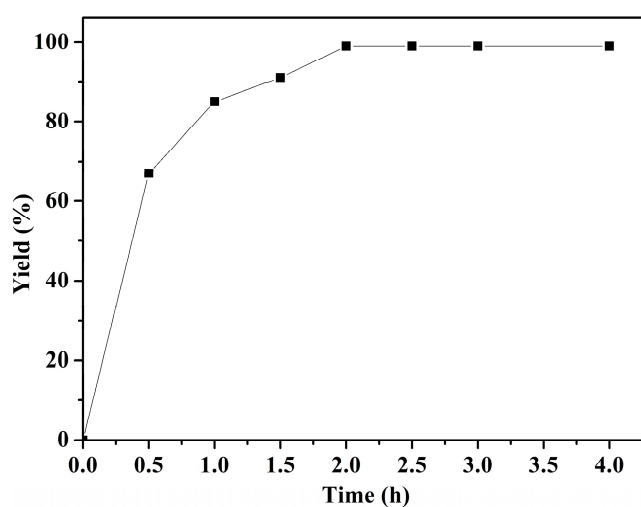


**Figure S20** The variation of 2-benzylidenemalononitrile yield with reaction time in H-UiO-66-(OAEAEAPTMS)<sub>2</sub>-based Pickering emulsion at 25°C

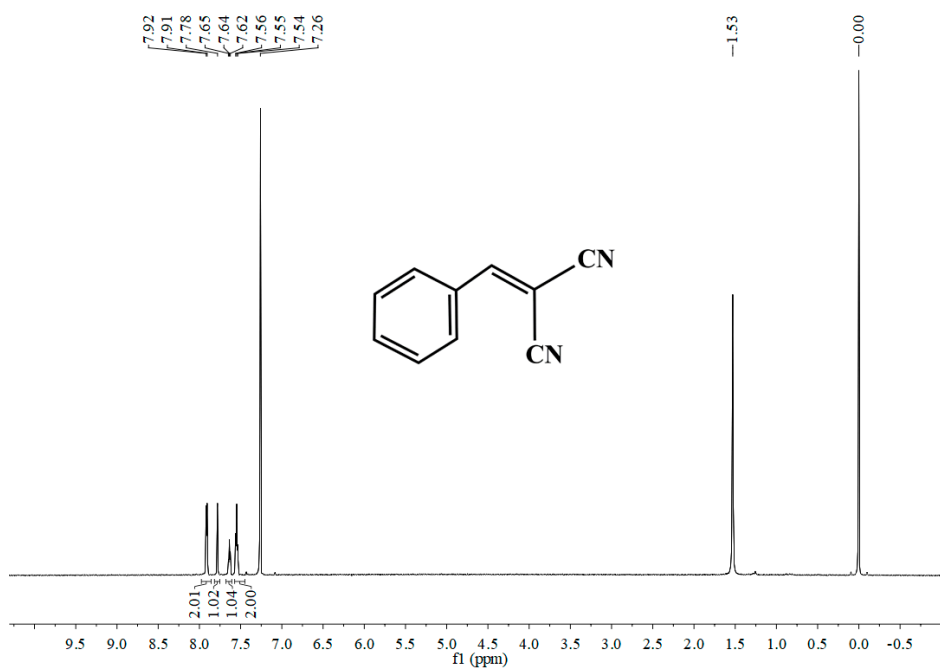


**Figure S21**  $^1\text{H}$  NMR of 2-benzylidenemalononitrile.

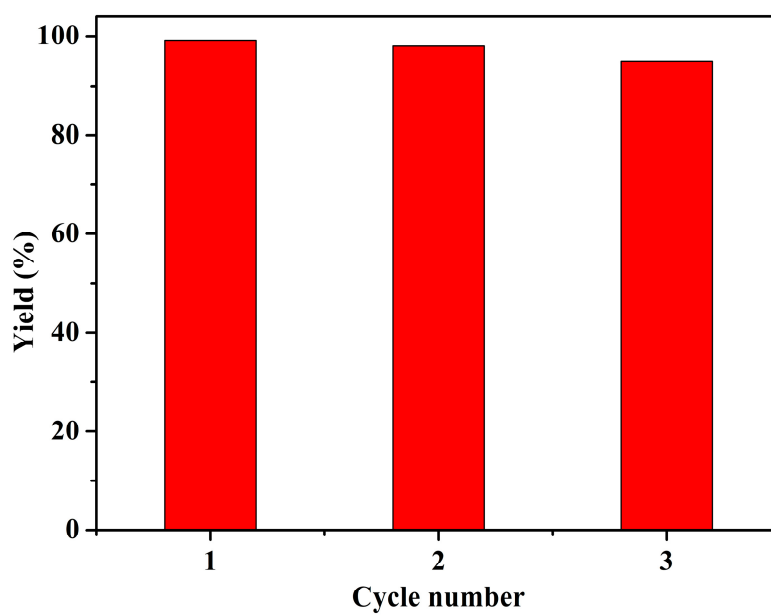


**Figure S22** The recyclability of Pickering emulsion in the reaction of benzaldehyde with malononitrile.

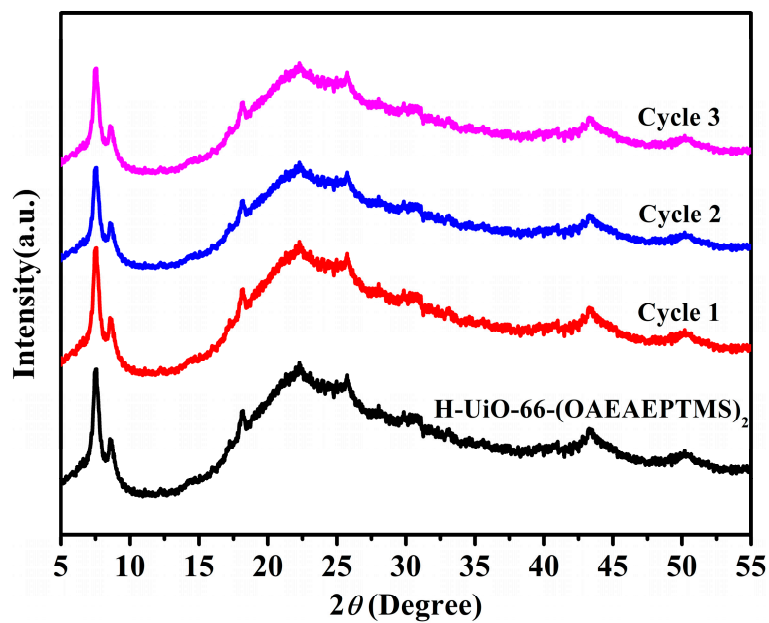


**Figure S23** PXRD patterns of H-UiO-66-(OAEAEPTMS)<sub>2</sub> before and after each catalytic run.

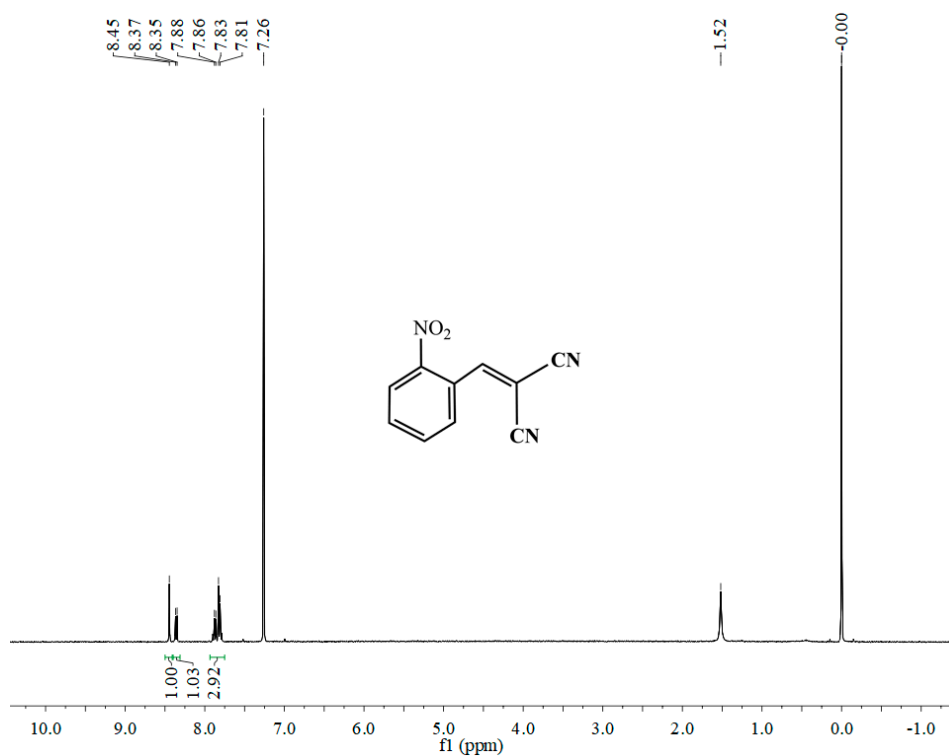


**Figure S24** <sup>1</sup>H NMR of 2-(2-nitrobenzylidene)malononitrile.

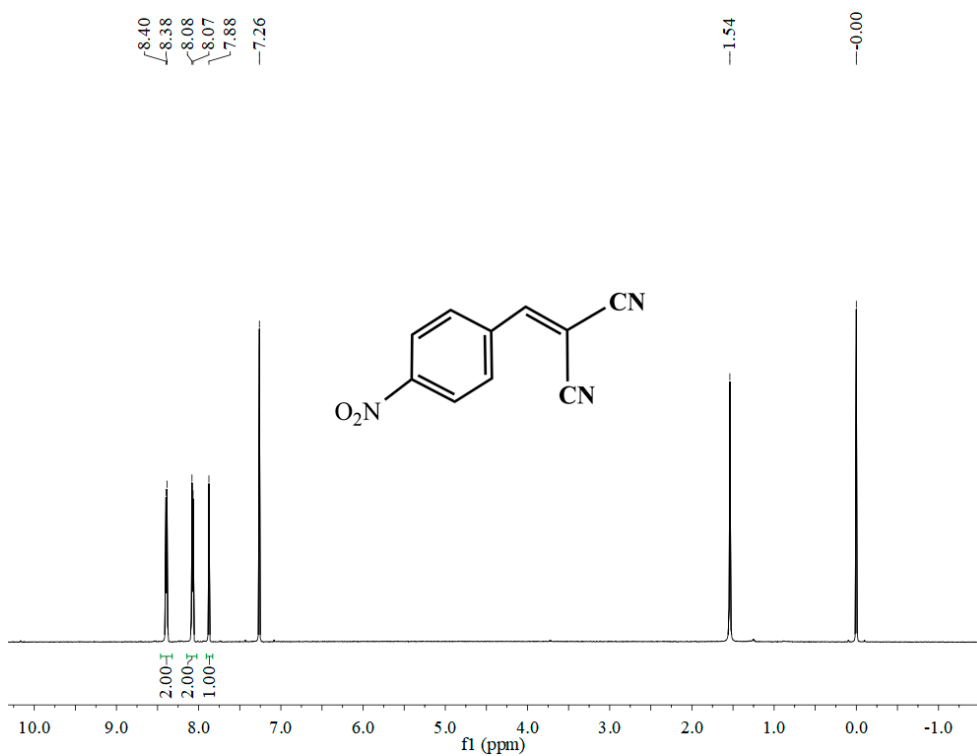


Figure S25  $^1\text{H}$  NMR of 2-(4-nitrobenzylidene)malononitrile.

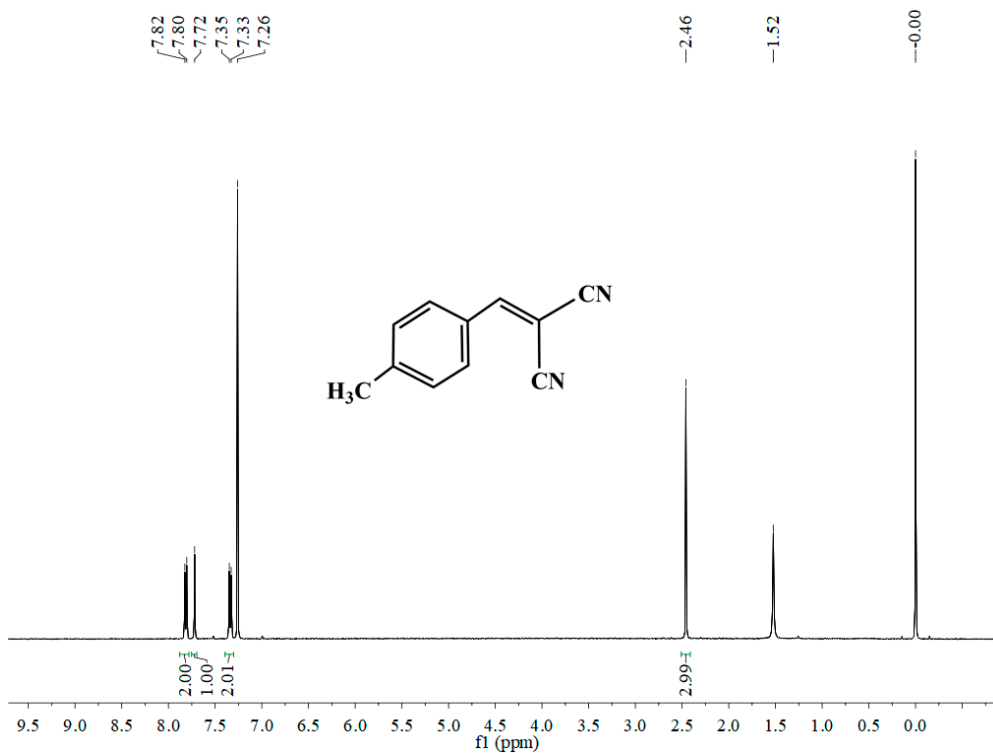
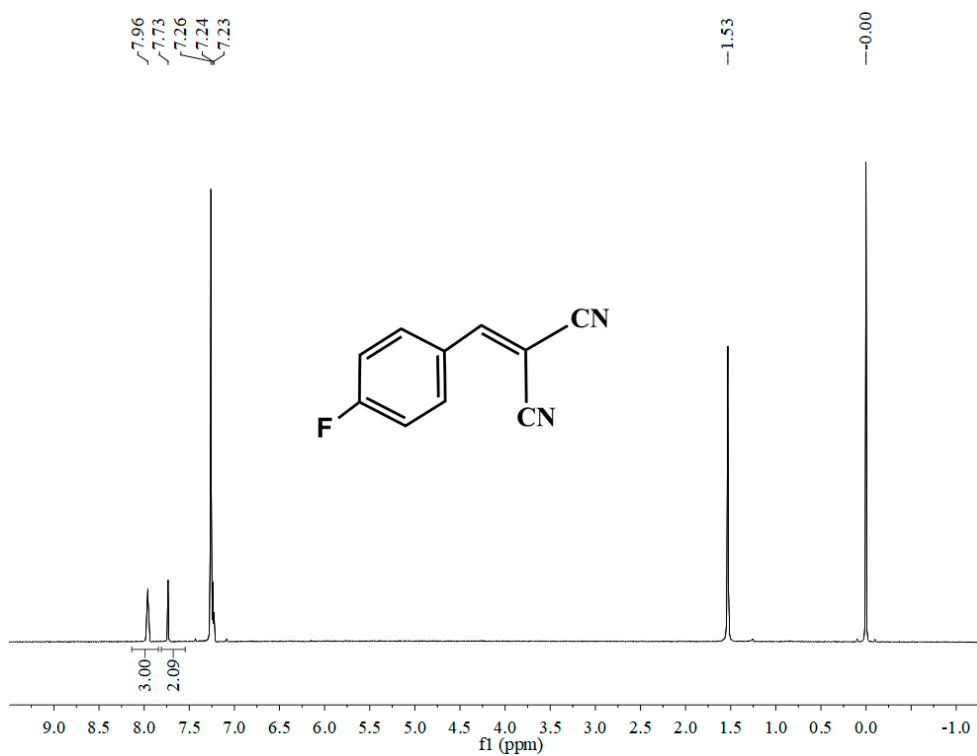
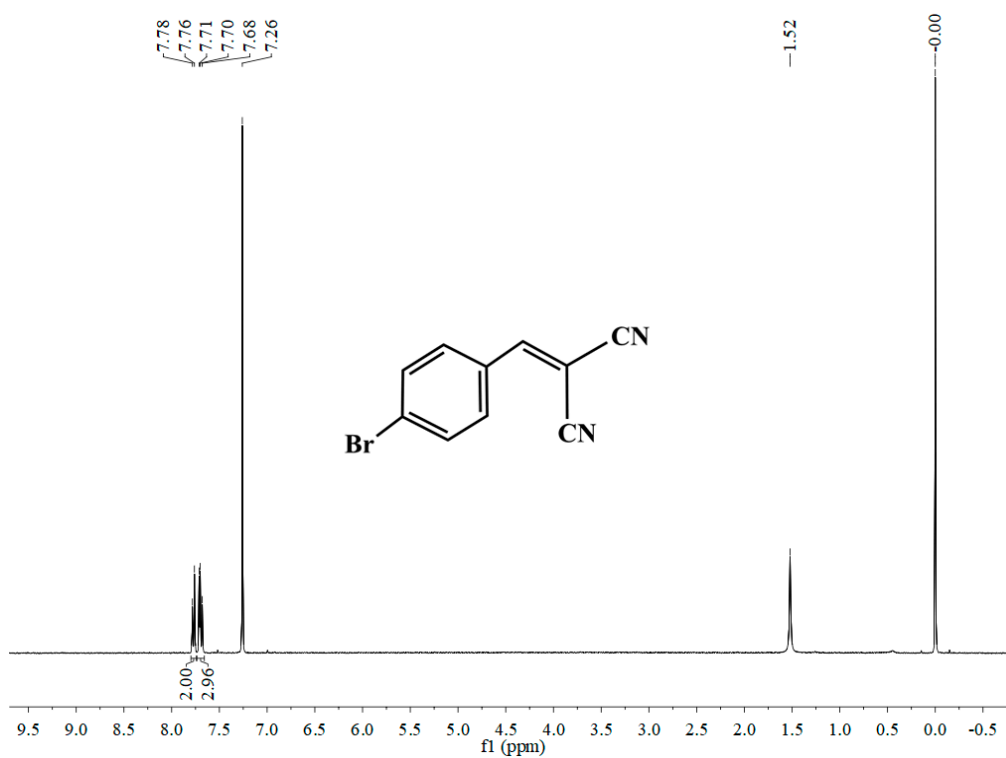


Figure S26  $^1\text{H}$  NMR of 2-(4-methylbenzylidene)malononitrile.



**Figure S27**  $^1\text{H}$  NMR of 2-(4-fluorobenzylidene)malononitrile.



**Figure S28**  $^1\text{H}$  NMR of 2-(4-bromobenzylidene)malononitrile.

### 3. Tables S1-S2

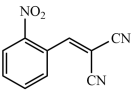
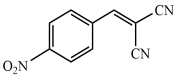
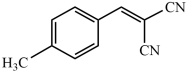
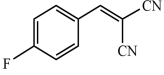
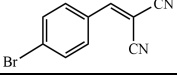
**Table S1** Surface chemical composition of the pristine and functionalized H-UiO-66-(OH)<sub>2</sub> (in at.%).

MOF	Zr	C	O	N	Si
H-UiO-66-(OH) <sub>2</sub>	1.24	84.43	14.34		
H-UiO-66-(OAPTMS) <sub>2</sub>	1.20	58.62	15.47	22.14	2.57
H-UiO-66-(OAEAPTMS) <sub>2</sub>	1.26	57.13	20.06	16.33	5.21
H-UiO-66-(OAEAEAPTMS) <sub>2</sub>	1.72	58.11	20.82	15.09	4.26

**Table S2** Reaction of benzaldehyde and malononitrile under different catalyst conditions.

Entry	Catalyst	GC Yield (%)
1	No	3
2	H-UiO-66-(OAPTMS) <sub>2</sub>	80
3	H-UiO-66-(OAEAPTMS) <sub>2</sub>	85
4	H-UiO-66-(OAEAEAPTMS) <sub>2</sub>	93

**Table S3.** Recyclability data of reaction of aldehydes and malononitrile under the same conditions.

Entry	Product	Cycle 1 (%)	Cycle 2 (%)	Cycle 3 (%)
1		99	98	98
2		99	98	98
3		98	97	96
4		64	62	61
5		74	72	72